



Variation in Articular Cartilage Thickness Among Extant Salamanders and Implications for Limb Function in Stem Tetrapods

Julia L. Molnar*

Department of Anatomy, New York Institute of Technology, College of Osteopathic Medicine, Old Westbury, NY, United States

OPEN ACCESS

Edited by:

Zerina Johanson,
Natural History Museum
(United Kingdom), United Kingdom

Reviewed by:

Pavel Skutschas,
Saint Petersburg State University,
Russia

Jürgen Kriwet,
University of Vienna, Austria

*Correspondence:

Julia L. Molnar
Julia.molnar@nyit.edu

Specialty section:

This article was submitted to
Paleontology,
a section of the journal
Frontiers in Ecology and Evolution

Received: 22 February 2021

Accepted: 19 April 2021

Published: 11 May 2021

Citation:

Molnar JL (2021) Variation
in Articular Cartilage Thickness
Among Extant Salamanders
and Implications for Limb Function
in Stem Tetrapods.
Front. Ecol. Evol. 9:671006.
doi: 10.3389/fevo.2021.671006

The size and shape of articular cartilage in the limbs of extant vertebrates are highly variable, yet they are critical for understanding joint and limb function in an evolutionary context. For example, inferences about unpreserved articular cartilage in early tetrapods have implications for how limb length, joint range of motion, and muscle leverage changed over the tetrapod water-land transition. Extant salamanders, which are often used as functional models for early limbed vertebrates, have much thicker articular cartilage than most vertebrate groups, but the exact proportion of cartilage and how it varies across salamander species is unknown. I aimed to quantify this variation in a sample of 13 salamanders representing a broad range of sizes, modes of life, and genera. Using contrast-enhanced micro-CT, cartilage dimensions and bone length were measured non-destructively in the humerus, radius, ulna, femur, tibia, and fibula of each specimen. Cartilage correction factors were calculated as the combined thickness of the proximal and distal cartilages divided by the length of the bony shaft. Articular cartilage added about 30% to the length of the long bones on average. Cartilage was significantly thicker in aquatic salamanders ($42 \pm 14\%$ in the humerus and 35 ± 8 in the femur) than in terrestrial salamanders ($21 \pm 7\%$ in both humerus and femur). There was no consistent relationship between relative cartilage thickness and body size or phylogenetic relatedness. In addition to contributing to limb length, cartilage caps increased the width and breadth of the epiphyses by amounts that varied widely across taxa. To predict the effect of salamander-like cartilage correction factors on muscle leverage, a simplified model of the hindlimb of the Devonian stem tetrapod *Acanthostega* was built. In this model, the lever arms of muscles that cross the hip at an oblique angle to the femur was increased by up to six centimeters. Future reconstructions of osteological range of motion and muscle leverage in stem tetrapods and stem amphibians can be made more rigorous by explicitly considering the possible effects of unpreserved cartilage and justifying assumptions based on available data from extant taxa, including aquatic and terrestrial salamanders.

Keywords: early tetrapods, salamanders, cartilage, soft tissue, joint, muscle leverage, *Acanthostega*, water-land transition

INTRODUCTION

Articular cartilage morphology in extant taxa has been used as a basis to infer the extent of unpreserved cartilage in fossils animals for the purpose of reconstructing joint and limb function (e.g., Hutchinson et al., 2005; Jannel et al., 2019; Tsai et al., 2020; Molnar et al., 2021). Articular cartilage seldom fossilizes, so its morphology in extant taxa may provide the best guide for reconstructing this tissue in extinct animals. Failure to account for unpreserved articular cartilage may result in underestimation of limb lengths and thus stride length and speed, as well as affecting joint congruence and thus posture and range of motion (Holliday et al., 2010). Furthermore, the amount of articular cartilage affects the relative position of muscle attachments, so assumptions about cartilage thickness will affect reconstructions of muscle leverage (Dao et al., 2020).

In the case of stem tetrapods, salamanders may provide the most informative extant model for articular cartilage. Salamanders are often used as models for limb-based locomotion in stem tetrapods because of their similar body proportions and amphibious lifestyle (Ashley-Ross, 2004; Kawano and Blob, 2013; Pierce et al., 2013). On a histological level, however, the analogy becomes more complicated, and some background in tetrapod bone development is necessary to understand the similarities and differences between and among the two groups. As in other vertebrates, ossification in the long bones of extant salamanders begins with a cartilaginous template, and bone is deposited around the periphery of the shaft (perichondral ossification), increasing the bone's diameter (Francillon-Vieillot et al., 1990). Simultaneously, the length of the bone is increased by periosteal bone deposited toward the epiphyses (Sanchez et al., 2010b). This epiphyseal cartilage hypertrophies and becomes calcified, and much of it is later resorbed to form the marrow cavity, which expands from the mid-shaft toward the epiphyses as the bone grows longer. Between the hypertrophic cartilage and the undifferentiated cartilage that will become the articular surface is a region of "seriated" or "stratified" cartilage in which the chondrocytes are organized in columns (Francillon-Vieillot et al., 1990). The erosion of the cartilage by the marrow forms a series of longitudinal projections called "marrow processes" within the hypertrophic cartilage (Haines, 1942). Medullary trabecula following the same longitudinal pattern as the chondrocytes are formed by endochondral ossification (Haines, 1942).

Although the basic processes of endochondral ossification are similar among tetrapods, there are several differences in the epiphyses of salamanders, some of which are shared with early vertebrates. First, secondary ossification centers do not develop in salamanders or in vertebrates close to the tetrapod water-land transition, such as the tetrapodomorph fish *Eusthenopteron* (Sanchez et al., 2014) and the limbed tetrapodomorph *Acanthostega* (Sanchez et al., 2016), or even in many stem amniotes (Sanchez et al., 2008). This similarity between salamanders and stem tetrapods is important for soft tissue reconstruction because articular cartilages in adult long bones are much thicker in animals that develop secondary centers of ossification (mammals and lepidosaurs) than in turtles, crocodylians, and salamanders, which do not (Haines, 1942; Xie

et al., 2020). Second, the columnar organization of the stratified cartilage is more pronounced in mammals and birds and less so in salamanders and turtles (Haines, 1942; Francillon-Vieillot et al., 1990), and in amphibians ossification does not occur in the stratified region (Estefa et al., 2021). Furthermore, in neotenic salamanders such as *Cryptobranchus* and *Proteus* the chondrocytes and the trabecula that replace them tend to be irregularly disposed without much organization at all (Haines, 1938, 1942). A similar condition was described in the facultatively neotenic, semi-aquatic newt *Pleurodeles waltl* (Quilhac et al., 2014). In contrast, a longitudinal arrangement of medullary trabecula has been described in stem tetrapods both with and without limbs (Sanchez et al., 2014, 2016; Kamska et al., 2018), suggesting that, like extant amniotes, their most likely mechanism of bone elongation is endochondral ossification of longitudinal columns of hypertrophic cartilage (Estefa et al., 2021). Third, in some neotenic salamanders such as *Proteus* endochondral ossification is minimal; the cartilage within the shaft persists, calcified cartilage is retained in the adult, and no primary medullary cavity is formed (Haines, 1938; Francillon-Vieillot et al., 1990). In this respect neotenic salamanders resemble stem tetrapods, which also lacked a central marrow cavity (Estefa et al., 2021).

Although bone structure in salamanders is well described, quantitative studies of articular cartilage in salamanders are rare. Descriptive studies of various species (von Eggeling, 1869; Klintz, 1912; Francis, 1934; Haines, 1938) illustrate ossified/calcified and cartilaginous epiphyses with a wide range of sizes, shapes and structures. Using contrast-enhanced micro-CT (DiceCT) to non-destructively visualize bone and cartilage morphology, I aimed to estimate variation among and identify correlates of articular cartilage thickness within extant salamanders. These results, in combination with fossil morphology, provide a basis for estimating how unpreserved articular cartilage affects reconstructions of joint range of motion and, particularly, muscle leverage in early limbed vertebrates.

MATERIALS AND METHODS

Specimens and Measurements

Salamander species were chosen to represent a wide range of genera (10), size (4.0–20.5 cm snout-vent length [SVL]), and mode of life (five aquatic, two semi-aquatic, and six terrestrial) (Table 1). All of the aquatic taxa were neotenic, having visible external gills and tailfins (Lynn, 1961; Wakahara, 1996), and all of the semi-aquatic and terrestrial taxa were fully metamorphosed. Seven specimens were scanned for this project, and an additional six DiceCT scans were downloaded from MorphoSource¹. DiceCT was chosen because it provides much better contrast and resolution (very important for small specimens) than traditional methods for measuring cartilage thickness such as CT, ultrasound, and MRI, and it is less destructive than anatomical sectioning. Nevertheless, only museum specimens available for destructive testing were

¹www.morphosource.org

TABLE 1 | Specimens and scanning.

Scientific name	Taxon		Specimen				Scanning		
	Adult habitat	Adult size/sexual maturity (cm)	Source	Number	SVL (cm)	Mass (g)	Source	Media ID	Resolution
<i>Pleurodeles waltl</i> *	Semi-aquatic (10)	11–30 total length (10)	AMNH	A-168418	3.7	2.21	NYIT		8.9
<i>Bolitoglossa porrasorum</i>	Terrestrial (3)	5.8–6.2 SVL (3)	UF	156522	4.4	-	MorphoSource	doi: 10.17602/M2/M43742	25.1
<i>Hynobius nebulosus</i>	Terrestrial (6)	4–7 SVL (6)	UF	24315	5.9	-	MorphoSource	ark:/87602/m4/M133947	22.1
<i>Pseudotriton ruber</i>	Aquatic and terrestrial (4)	5.5 SVL (4)	NYIT	MG-1257	6.1	6.56	NYIT		12.9
<i>Plethodon cinereus</i>	Terrestrial (4)	3.2–4.1 SVL (4)	AMNH	A-159522	4.0	1.02	NYIT		7.1–5.7
<i>Ambystoma tigrinum</i> *	Terrestrial (not neotenic) (4)	7.6–16.5 SVL (2)	AMNH	FS-26619	6.6	11.81	NYIT		19.9
<i>Ambystoma maculatum</i>	Terrestrial (4)	5.6–7.8 SVL (4)	UF	26607	7.6	-	Morpho-source	ark:/87602/m4/M141549	35.3
<i>Salamandria salamandra</i>	Terrestrial (8)	9.4–10.6 total length (7)	AMNH	FS-26618	7.7	15.3	NYIT		27.9
<i>Ambystoma mexicanum</i>	Aquatic (3)	15–45 total length (9)	AMNH	A-144861	10.1	69.91	NYIT		27.1
<i>Siren intermedia</i>	Primarily aquatic (4)	15–18 SVL (4)	UF	123993	13.2	-	MorphoSource	ark:/87602/m4/M141555	46.8
<i>Siren lacertina</i>	Aquatic (4)	50–98 total length (6)	AMNH	A-171810	15.4	79.08	NYIT		25
<i>Cryptobranchius alleganiensis</i>	Aquatic (4)	30–40 total length (4)	UF	10881	16.0	-	MorphoSource	ark:/87602/m4/M67234	67.6
<i>Necturus maculatus</i>	Aquatic (4)	17.5–20 total length (4)	AMNH	FS-26617	20.5	123.62	NYIT		32.5–33.9

References: 1 (Nafis, 2018), 2 (Rafaeli, 2014), 3 (Lannoo, 2005), 4 (Petranka, 1998), 5 (Goris and Maeda, 2005), 6 (Najibar et al., 2020), 7 (AmphibiaWeb, 2020), 8 (Helmenstine, 2020), and 9 (Joven et al., 2015). *Indicates specimens with unilateral broken or missing limb(s). SVL, snout-vent length; AMNH, American Museum of Natural History; NYIT, New York Institute of Technology; UF, University of Florida. MorphoSource: University of Florida provided access to these data, the collection of which was funded by oVert TCN; NSF DBI-1701714. The files were downloaded from www.MorphoSource.org, Duke University.

used because of concerns about damage resulting from the contrast staining procedure. All specimens had been preserved in ethanol. Specimens were stained by immersion in 9% potassium iodide solution for approximately 2 weeks (Metscher, 2009). After staining, they were imaged using a Skyscan 1173 high-energy desktop micro-CT scanner (www.skyscan.be) at 8–35 μm resolution. Scans were reconstructed in NRecon software².

Reconstructed scans were imported into Amira2020.2 software³. The contrast medium made it possible to visually distinguish between mineralized tissue, cartilage, and other soft tissues in the scans (Figures 1A–D). Proximal cartilage cap, bony shaft, and distal cartilage cap of each humerus, femur, radius, and ulna were semi-automatically segmented (in the two *Siren* species, only the forelimb elements were present) (Figures 1E–H). Length of each element was measured using the 3D measure tool in Amira (Figure 1I, Table 2). Some specimens had concave mineralized epiphyses with tapering cartilage cones that extended toward the marrow cavity (arrows in Figures 1A,B). In these specimens, measurements of cartilage thickness did not include the portion sheathed in bone because this portion would not affect the length of the limb element or the shape of its articular surface. However, cartilage within the shaft would affect the material properties of the limb. Measurements were taken bilaterally from the humerus and femur in specimens with four intact limbs (see Table 1). In addition, length of the long and short axes of the mineralized and cartilaginous epiphyses of the humerus and femur was measured unilaterally (Figures 1J,K).

Statistical Analysis

Statistical analyses were performed in SPSS version 27. Cartilage thickness as a percentage of bone length (“cartilage correction factor” or CCF, sensu Holliday et al., 2010) was calculated as the sum of the thickness of the proximal and distal cartilages divided by the length of the bony shaft (because it is a ratio, CCF is independent of body size). Taxa were coded as terrestrial, semi-terrestrial, or aquatic based on descriptions from the literature (Table 1).

Three hypotheses were tested: 1) mean cartilage correction factors for the humerus and femur are significantly different between aquatic and terrestrial taxa, 2) the humerus and femur contain a similar proportion of cartilage, and 3) mean cartilage correction factor is not correlated with body size. To test hypothesis 1, independent-samples *T*-tests were conducted with CCF as the test variable and habit (terrestrial or aquatic) as the grouping variable. To meet the assumption of independent samples, left and right limbs were averaged and the humerus and femur were analyzed separately. Semi-aquatic salamanders were excluded from this analysis because there were only two taxa; i.e., not enough for a robust test. To test hypothesis 2, an additional independent-samples *T*-test was conducted with CCF as the test variable and bone (humerus or femur) as the grouping variable. Parametric tests were used because samples

²www.microphotonic.com

³www.thermofisherscientific.com

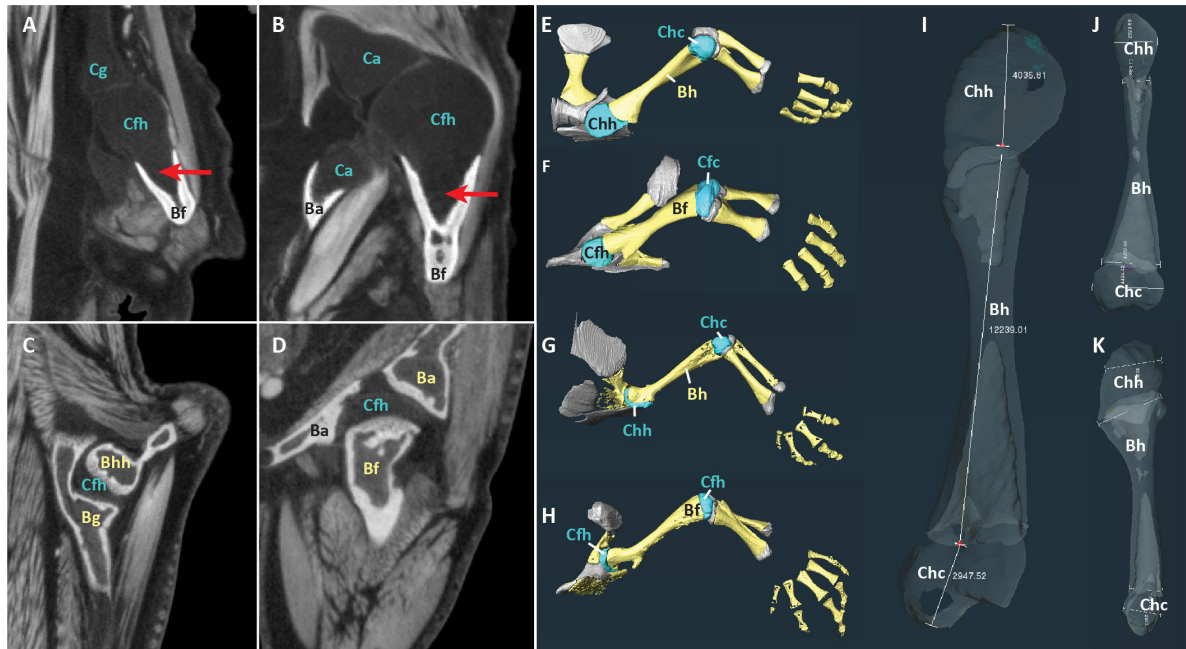


FIGURE 1 | Scans of representative aquatic and terrestrial salamanders showing morphological differences and measurement methods. **(A–D)** DiceCT slices through shoulder **(A)** and hip **(B)** joints of the aquatic salamander *Necturus maculatus* and the shoulder **(C)** and hip **(D)** joints of the terrestrial salamander *Pseudotriton ruber*. Red arrows show cartilage cones within bony shaft. **(E–H)** 3-D surfaces of bones (yellow) and cartilages (blue and gray) in the forelimb of *N. maculatus* **(E)**, the hindlimb of *N. maculatus* **(F)**, the forelimb of *P. ruber* **(G)**, and the hindlimb of *P. ruber* **(H)** (carpals not shown). **(I–K)** Humerus of *N. maculatus* showing linear measurements in μm of cartilage thickness and bony shaft **(I)** and the long and short axes of the mineralized and cartilaginous epiphyses **(J,K)**. Abbreviations: bony acetabulum (Ba), bony femoral shaft (Bf), bony glenoid (Bg), bony humeral shaft (Bh), cartilaginous acetabulum (Ca), cartilaginous femoral condyles (Cfc), cartilaginous femoral head (Cfh), cartilaginous glenoid (Cg), cartilaginous humeral condyles (Chc), cartilaginous humeral head (Chh).

within each group did not violate the assumptions of normality (assessed using Shapiro–Wilk test). Significance levels were adjusted appropriately if data violated the assumption of equal variance under Levene’s Test. To test hypothesis 3, a Pearson product-moment correlations coefficient was computed to assess the relationship between CCF in the humerus and femur and snout-vent length.

Testing for Phylogenetic Signal

Ancestor reconstruction was performed in Mesquite 3.6⁴ using the maximum parsimony method and a time-calibrated phylogeny from TimeTree (timetree.org; Hedges et al., 2006). Seven characters were traced: average CCF for humerus and femur and individual CCFs for humerus, femur, radius, ulna, tibia, and fibula. The “phylosig” function in R (Revell, 2012) was used to test for phylogenetic signal in average CCF for the humerus and femur. A second test was conducted using alternative divergence times (Marjanovič and Laurin, 2014).

Moment Arm Analysis

To predict the effect of unpreserved articular cartilage on reconstructions of muscle leverage, two-dimensional muscle

moment arms were calculated using a custom script in MATLAB⁵ (Supplementary Table 1). The inputs were CCF and XY coordinates of the origin and insertion of each muscle relative to the joint center of rotation. For simplicity, the limb was assumed to be in a horizontal position. Outlines of the pelvis and femur of the stem tetrapod *Acanthostega* (Coates, 1996) were added for visualization purposes. *Acanthostega* was chosen because it is, along with *Ichthyostega*, the earliest limbed vertebrate represented by extensive post-cranial material (Clack, 2012), and because limb range of motion and muscle leverage have been reconstructed in this animal (Dao et al., 2020; Molnar et al., 2021). Basic graphing functions were used to calculate the moment arm: first, the equation of a line representing the muscle’s line of action relative to the joint center (set at the origin of the plot) was calculated, then a line was plotted perpendicular to the line of action and passing through the origin, and finally the distance between the origin and the intercept of the two lines (the moment arm). The insertion point was adjusted by the CCF, and the moment arm calculation was repeated. The muscles used in this example are abstractions used to demonstrate the range of effect sizes. However, the same code could be used to predict the effects of a particular CCF on a biologically realistic muscle using origin and insertion coordinates from an anatomically accurate illustration or model.

⁴mesquiteproject.org

⁵mathworks.com

TABLE 2 | Measurements of cartilage thickness and bony shaft length taken from humerus and femur (μm) and calculated percentage of humerus or femur length composed of cartilage.

Species	Humerus				Femur			
	Proximal cartilage	Distal cartilage	Bony shaft	CCF	Proximal cartilage	Distal cartilage	Bony shaft	CCF
<i>Ambystoma maculatum</i>	370	720	8,930	12.2%	720	280	8,990	11.1%
	350	600	9,030	10.5%	710	340	8,930	11.8%
<i>Ambystoma mexicanum</i>	1774.37	1438.27	13204.18	24.3%	2248.86	1307.71	13992.4	25.4%
	1795.32	1310.64	13037.12	23.8%	2311.5	1277.75	13935.68	25.8%
<i>Ambystoma tigrinum</i>	1365.61	1066.72	10110.05	24.1%	1275.82	836.35	8513.98	24.8%
<i>Bolitoglossa porrasorum</i>	-	-	-	-	-	-	-	-
	420	1,020	4,550	31.6%	580	950	4,620	33.1%
<i>Cryptobranchus alleganiensis</i>	390	940	4,570	29.1%	570	860	4,680	30.6%
	3,150	3,150	12,730	49.5%	2,980	1,970	14,020	35.3%
<i>Hynobius nebulosus</i>	2,990	3,290	12,900	48.7%	2,520	2,460	13,160	37.8%
	560	530	6,640	16.4%	480	350	6,190	13.4%
<i>Necturus maculatus</i>	480	650	6,600	17.1%	600	340	6,250	15.0%
	4035.81	2947.52	12239.01	57.1%	3683.7	1838.98	13288.84	41.6%
<i>Plethodon cinereus</i>	3846.77	2862.33	12091.66	55.5%	3583.38	1972.53	13457.88	41.3%
	71.23	441.74	2954.41	17.4%	308.45	327.45	3077.7	20.7%
<i>Pleurodeles waltl</i>	72.89	456.34	2930.93	18.1%	311.57	306.11	3090.32	20.0%
	931.88	1542.45	4732.74	52.3%	719.47	1289.93	4599.83	43.7%
<i>Pseudotriton ruber</i>	-	-	-	-	-	-	-	-
	332.7	889.09	5567.48	21.9%	451.74	605.3	6312.44	16.7%
<i>Salamandra salamandra</i>	283.4	914.86	5566.26	21.5%	461.65	605.57	6220.99	17.2%
	815.45	1877.5	10911.9	24.7%	1358.82	948.22	11017.1	20.9%
<i>Siren intermedia</i>	870.27	1756.52	11000.66	23.9%	1485.07	1000.03	10766.16	23.1%
	1,200	1,210	4,720	51.1%	-	-	-	-
<i>Siren lacertina</i>	1,240	1,120	4,720	50.0%	-	-	-	-
	1520.28	1335.4	8701.9	32.8%	-	-	-	-
	1309.08	1258.89	8861.18	29.0%	-	-	-	-

RESULTS

Among the taxa measured, articular cartilage added approximately 25–30% to the length of the humerus and femur on average (Figure 2). Cartilage made up a similar proportion of the distal limb bones (radius, ulna, tibia, and fibula). Relatively thicker cartilage caps were found in larger, more aquatic taxa, whereas phylogenetic relatedness did not predict relative cartilage thickness. The unexpected finding of thicker cartilage in larger taxa likely is related to the correlation of large body size with aquatic mode of life. Differences between forelimb and hindlimb and between proximal and distal cartilages were relatively small (about 5% on average), and the magnitude and direction of these differences were inconsistent across taxa (Table 2). In addition to contributing to the length of the humerus and femur, cartilages increased the dimensions of the articular surfaces in most salamanders.

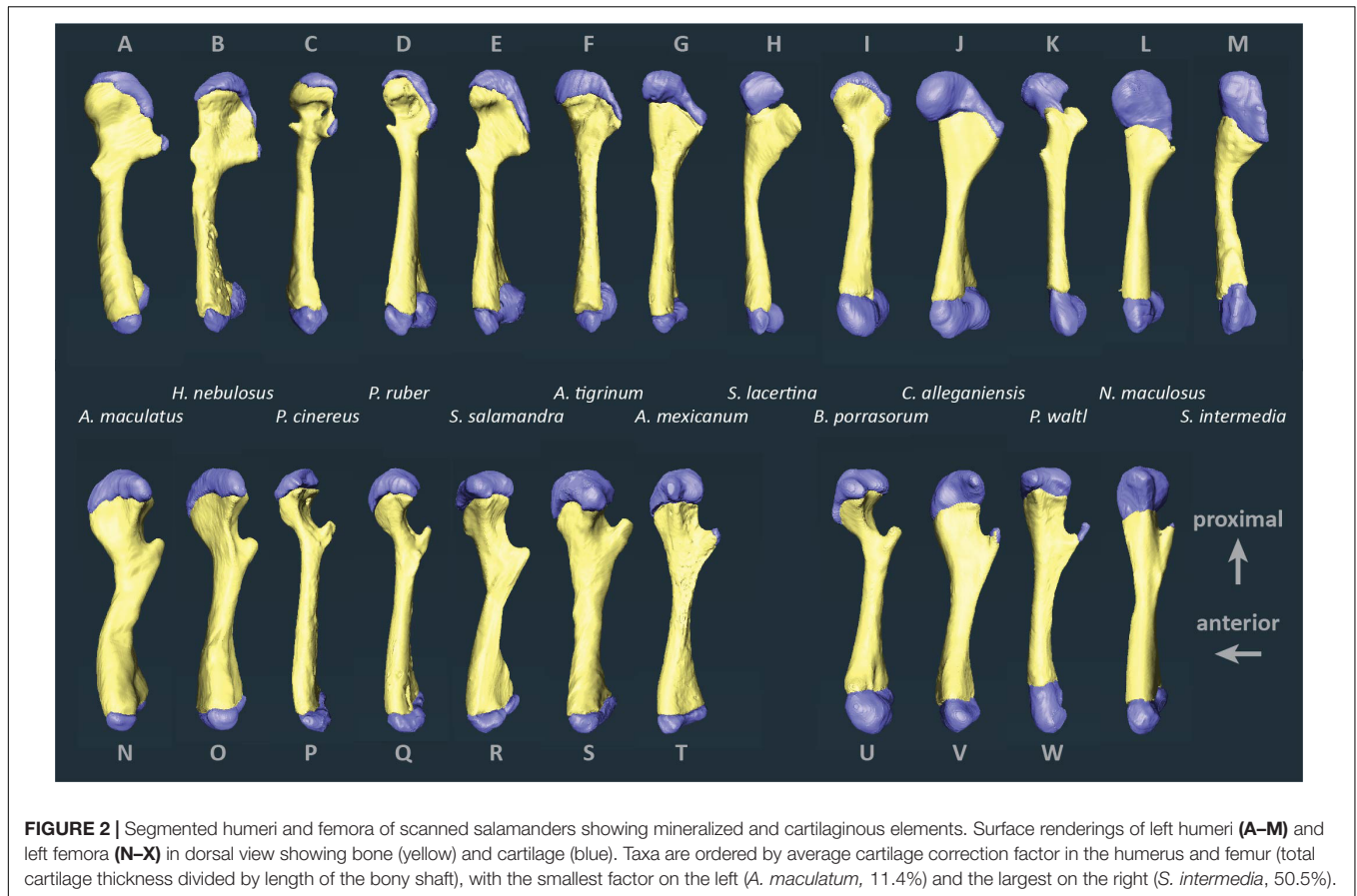
Qualitative Results

Articular cartilage was visible in both ends of each long bone and, in some specimens, at the tip of the greater trochanter of the femur (Figure 2). Two different epiphyseal structures were identifiable: one with concave mineralized epiphyses in which

the cartilage cap continued toward the midpoint of the shaft, and one with flat or convex epiphyses in which the cartilage cap was clearly separated from the marrow cavity (compare Figures 1A–D). The first type was mainly found in aquatic taxa with relatively thick cartilage (*N. maculatus*, *C. alleganiensis*, *P. waltl*, *S. lacertina*, and *S. intermedia*).

Differences Within Individuals

The humerus contained slightly more cartilage than the femur on average, but the difference was not statistically significant (Figure 3, Table 2). The 13 humeri ($M = 31.4\%$, $SD = 15.3\%$) compared to the 11 femora ($M = 26.3\%$, $SD = 10.8\%$) had non-significantly thicker articular cartilage, $t(22) = 0.94$, $p = 0.184$. In six taxa the cartilages in the humerus were noticeably thicker (particularly *Cryptobranchus*, which had unusually thick cartilages on the distal end of the humerus), and in five taxa the cartilages in the femur were slightly thicker (Figure 2, Table 2). Thickness of proximal and distal cartilage caps (humeral condyles) was similar on average, except that the distal caps on the humerus were slightly thicker than in the other three locations ($17.5 \pm 7.5\%$ versus $12.3 \pm 14.0\%$; Table 2). Individual taxa showed much greater differences; for example, in the femur of *Necturus maculatus* the proximal cartilage caps were twice as

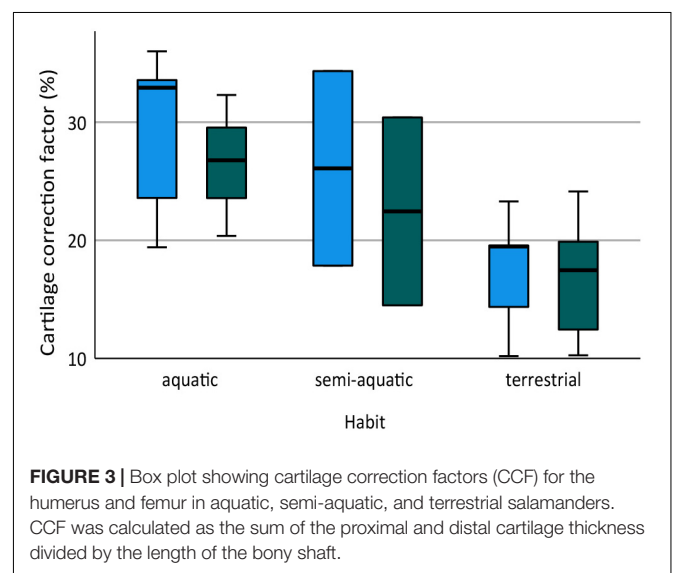


thick as the distal caps, whereas in the humerus of *Plethodon cinereus* the distal cartilages were six times as thick as the proximal ones (Figure 2, Table 2). Some left-right asymmetry was observed: 5–8% in the thickness of cartilage caps, but only 1–2% in the bony shafts (Table 2). This discrepancy may indicate a biological difference or it may reflect measurement error, segmentation error, and/or cartilage deformation in preserved specimens. However, because CCF is expressed as a percentage of the length of the shaft, even a 10% difference in cartilage thickness would change CCF by only about 3–5%.

The distal elements contained a similar proportion of cartilage to the humerus and femur. Among the limb bones, the thickest articular cartilage was found in the proximal end of the ulna where it made up most of the olecranon process (27.9% bone length on average; Table 3). The thinnest cartilages on average were found in the proximal ends of the radius and tibia (8.7–10.1%). Because of the large olecranon cartilage, the cartilage correction factor was greatest in the ulna (44.1% bone length on average versus 25–29% in the radius, tibia, and fibula).

Body Size and Terrestriality

Aquatic salamanders had significantly thicker articular cartilage in the humerus and femur than terrestrial salamanders (Figure 3). In the humerus, the five aquatic salamanders ($M = 42.2\%$, $SD = 13.9\%$) compared to the six terrestrial



salamanders ($M = 20.7\%$, $SD = 6.8\%$) had significantly thicker articular cartilage, $t(6) = 3.2$, $p = 0.022$ (equal variances not assumed). In the femur, the three aquatic salamanders with hindlimbs ($M = 34.5\%$, $SD = 8.1\%$) compared to the six terrestrial salamanders ($M = 20.8\%$, $SD = 7.4\%$) had significantly

TABLE 3 | Measurements of cartilage thickness and bony shaft length taken from radius, ulna, tibia, and fibula (μm) and calculated cartilage correction factors for each bone (CCF).

Species	Radius			Ulna			Tibia			Fibula		
	Proximal cartilage	Bony shaft	Distal cartilage	Proximal cartilage	Bony shaft	Distal cartilage	Proximal cartilage	Bony shaft	Distal cartilage	Proximal cartilage	Bony shaft	Distal cartilage
<i>Ambystoma maculatum</i>	0	4,250	360	410	5,710	420	220	5,310	380	200	5,170	420
<i>Ambystoma mexicanum</i>	801.83	7478.12	518.44	799.16	7088.53	314.2	519.25	8939.05	956.5	913.17	7829.97	791.32
<i>Ambystoma tigrinum</i>	406.57	5326.73	632.55	1022.28	6118.79	502.04	487.32	5071.31	1130.92	763.84	4905.63	488.81
<i>Bolitoglossa porrasorum</i>	240	2,870	500	600	2,810	510	350	2,880	530	480	2,820	460
<i>Cryptobranchius alleganiensis</i>	780	6,250	1,560	3,260	6,060	1,170	1,260	7,100	1,790	1,060	6,670	1,860
<i>Hynobius nebulosus</i>	140	3,340	430	740	3,680	380	210	3,710	240	370	3,360	410
<i>Necturus maculatus</i>	612.49	5963.49	896.71	2763.62	6303.57	928.72	962.09	5649.33	894.47	878.86	5383.92	791.13
<i>Pleurodeles cinereus</i>	50.93	1683.86	264.23	168.35	1749.13	182.26	103.39	1811.57	249.46	96.41	1790.98	208.91
<i>Pleurodeles waltl</i>	223.35	2311.99	726.27	1027.87	2304.02	592.77	457.53	2174.14	494.18	618.47	2201.51	663.23
<i>Pseudotriton ruber</i>	158.08	3146.07	662.53	472.88	2967.95	468.44	229.48	3533.1	498.76	431.24	3388.58	367.4
<i>Salamandria salamandra</i>	339.2	6205.67	880.66	1489.92	5910.92	943.32	429.45	5690.47	633.11	714.73	5432.4	819.66
<i>Siren intermedia</i>	540	2,010	770	1,260	2,310	540						
<i>Siren lacertina</i>	456.64	4216.73	942.49	1805.89	4249.25	981.96						
Average	365.31	4234.82	703.38	1216.92	4403.24	610.29	475.32	4715.36	708.85	593.34	4450.27	661.86

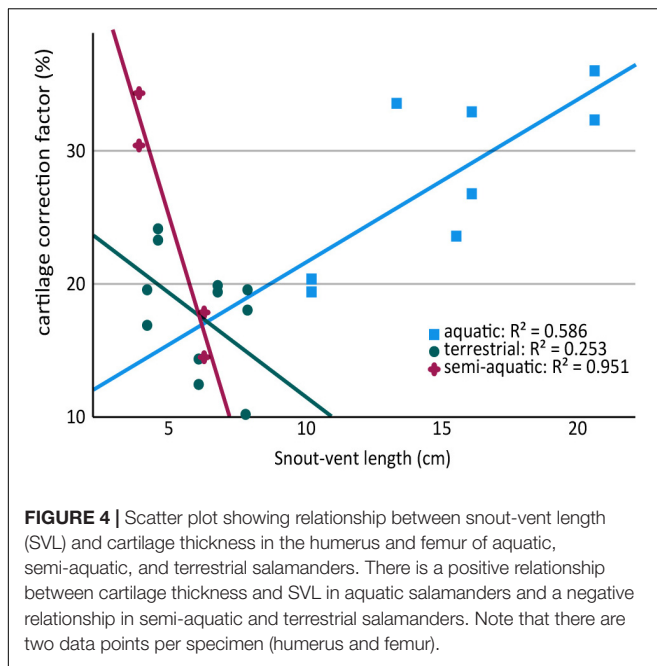
thicker articular cartilage, $t(7) = 2.6$, $p = 0.037$. The thickest cartilages (>45% bone length) were found in large aquatic salamanders: the mudpuppy *N. maculatus* (41.3–57.1%), the limb-reduced *S. intermedia* (50.0–51.1% in the forelimb), the giant salamander *C. alleganiensis* (35.3–49.5%), and the semi-aquatic newt *P. waltl* (43.7–52.3%) (Table 2). Qualitatively, the salamanders with the thickest cartilage (*N. maculatus*, *C. alleganiensis*, *P. waltl*, and both *Siren* species) lacked ossified or calcified epiphyses, and cones of cartilage extended deep to the cortical bone within the diaphysis (see Figures 1A,B). The thinnest cartilages (<22%) were found in the small to medium-sized terrestrial salamanders *A. maculatum* (10.5–12.2%), *H. nebulosus* (13.4–17.1%), *P. cinereus* (16.5–20.7%), and *P. ruber* (16.7–21.9%). Intermediate amounts of cartilage (23–35%) were found both in aquatic salamanders (*A. mexicanum* [23.8–25.8%] and *S. lacertina* [29.0–32.8%]) and terrestrial salamanders (*S. salamandra* [20.9–25.1%], *A. tigrinum* [24.1–24.8%], and *B. porrasorum* [29.1–33.1%]).

A similar relationship between cartilage thickness and terrestriality was found in the radius, ulna, tibia, and fibula. The thickest cartilages were found in *S. intermedia* (71.5% bone length), *P. waltl* (53.4%), *S. lacertina* (49.4%), *C. alleganiensis* (49.3%), and *N. maculatus* (36.9%) and the thinnest in *A. maculatum* (11.6%), *A. mexicanum* (17.9%), *P. cinereus* (18.8%), and *H. nebulosus* (20.7%). The most notable difference was *S. lacertina*, which had an intermediate proportion of cartilage in the humeri (similar to *B. porrasorum*) but a large proportion in the radius and ulna (similar to *C. alleganiensis*).

Because aquatic salamanders tend to be larger, it is difficult to examine the effects of body size separately from mode of life. Cartilages were thicker in larger salamanders in this study (a positive correlation between CCF and SVL), and the correlation was statistically significant in the humerus ($r = 0.577$, $n = 13$, $p = 0.036$) though not in the femur ($r = 0.499$, $n = 11$, $p = 0.118$). However, the effect disappeared when salamanders were separated by mode of life: among aquatic salamanders there was a positive correlation between SVL and relative cartilage thickness, but among terrestrial and semi-aquatic salamanders the correlation was negative (Figure 4). Within the sample there was no overlap in size between aquatic salamanders (>10 cm SVL) and terrestrial salamanders (<8 cm SVL). Because mode of life was a far better predictor of cartilage thickness than body size was, and because there is no reason to expect that larger animals would have thicker cartilages, the most likely explanation is that the positive relationship between body size and CCF is an artifact of the relationship between body size and mode of life. A larger, more extensive sample would be required to verify or exclude a relationship between relative cartilage thickness and body size.

Phylogenetic Relatedness

No phylogenetic signal was detected in the average CCFs for the humerus and femur (Blomberg's $K = 0.271$, $p = 0.355$), and no phylogenetic pattern was apparent in the ancestor reconstruction (Figure 5). Large variations were present within genera: among the three *Ambystoma* species, cartilage correction factors in the humerus and femur ranged from very small in *A. maculatum* (11.4%) to medium in *A. mexicanum* and



A. tigrinum (24.4–24.8%), and between the two *Siren* species from medium in *S. lacertina* (30.9%) to large in *S. intermedia* (50.1%). Ancestor reconstruction showed intermediate values at the nodes leading to the three major clades: Cryptobranchoidea (30.7%), Salamandroidea (31.8%), and Sirenidae (40.6%) (Figure 5). Separate ancestor reconstructions on each individual bone yielded similar results (Supplementary Data Sheet 1). A second analysis using divergence times from a more recent timetree (Marjanović and Laurin, 2014) also failed to detect a phylogenetic signal (Blomberg's $K = 0.259$, $p = 0.309$).

Dimensions of Articular Surfaces

The dimensions of the cartilaginous epiphyses were greater than their mineralized (ossified or calcified) equivalents in most cases, and in many their proportions were substantially different. Like the thickness of articular cartilages, the magnitude of the differences between dimensions of cartilaginous and mineralized epiphyses appear to be related to mode of life. The smallest cartilage correction factors on average (<15%) were found in semi-aquatic and terrestrial salamanders (*A. maculatum*, *H. nebulosus*, *P. ruber*, and *P. cinereus*) and the largest (>30%) were found in aquatic and semi-aquatic ones (*P. waltl* and *N. maculatus*). There were also noticeable differences between the humerus and femur, and between the proximal and distal cartilages. In the humerus, the cartilaginous epiphyses were more spherical than their mineralized counterparts: cartilage added 24.8–27.8% on average to the short axes of the humeral head and condyles but only 11.1–17.4% to their long axes (Table 4). In the femur the average increase was similar in both dimensions, resulting most commonly in an increase in size without a change in shape. However, in the femur there was a big difference in CCF between the femoral head and the condyles (+29.8% versus +13.9% on average). There was a lot of variation within each

group and quite a bit of overlap between aquatic and terrestrial taxa, so it would be difficult to predict the shape of articular cartilage based on mineralized epiphyses in salamanders.

DISCUSSION

Salamanders often are used as extant models for early limbed vertebrates, so the range, variability, and correlates of articular cartilage thickness in salamanders will affect inferences about limb function over the tetrapod water–land transition. Because ossification of the tetrapod postcranial skeleton is thought to be functionally related to gravitational forces encountered during terrestrial locomotion (e.g., Carter et al., 1998), and because the effect of gravity scales proportionally with body mass, I predicted that the percentage of cartilage would be greater in smaller and more aquatic salamanders. This prediction was partially borne out by the data: no consistent relationship was observed between cartilage thickness and size (quantified by snout-vent length), but the proportion of cartilage was significantly greater in aquatic salamanders than terrestrial ones. No obvious phylogenetic pattern was observed. The results were applied to a mathematical model of the hip joint of a limbed Devonian tetrapodomorph, demonstrating that salamander-like articular cartilage would have substantially increased the leverage of muscles that cross the hip at an oblique angle to the femur. These results emphasize the importance of articular cartilage for reconstruction of limb length, range of motion, and muscle leverage in extinct tetrapods such as early salamanders and stem tetrapods and provide an empirical starting point to account for these effects.

Limitations

Much of the observed variation in articular cartilage thickness could not be explained by terrestriality alone. For example, the Spotted Salamander *A. maculatum* had much less cartilage in the humerus and femur than the other terrestrial taxa (only about 10% of each element). To my knowledge, there is nothing about the species or specimen to suggest that it should have an unusually small amount of cartilage. Another member of the genus, the Axolotl *A. mexicanum*, also had much less cartilage in the humerus and femur than would be predicted by mode of life (19–21%, compared with an average of 35–42% among all aquatic salamanders). It is possible that these results reflect a small phylogenetic effect that is masked by mode of life, and that *Ambystoma* species tend to have relatively less cartilage than other genera. Alternatively, the relatively thin cartilage in *A. mexicanum* may be attributed to metamorphic plasticity in this species: unlike the other “aquatic” taxa in this sample, metamorphosis can be hormonally induced in *A. mexicanum* (Wakahara, 1996). In addition, relative cartilage thickness was very different between the two semi-aquatic species: with a CCF of 44–52% in the humerus and femur, the Iberian Ribbed Newt *P. waltl* falls in the middle of the range of aquatic salamanders, whereas the Red Salamander *P. ruber*, at 17–22%, falls in the middle of the range of terrestrial salamanders. However, the unexpectedly large CCF in *P. waltl* might be explained by sexual maturity (see below). Finally, although the two species

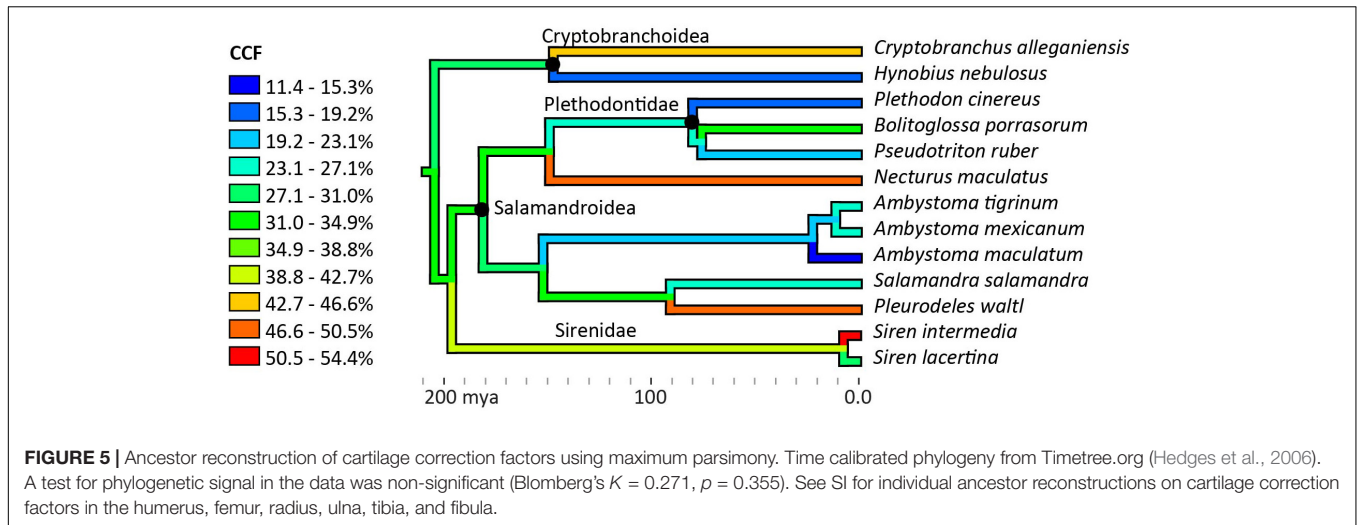


FIGURE 5 | Ancestor reconstruction of cartilage correction factors using maximum parsimony. Time calibrated phylogeny from Timetree.org (Hedges et al., 2006). A test for phylogenetic signal in the data was non-significant (Blomberg's $K = 0.271$, $p = 0.355$). See SI for individual ancestor reconstructions on cartilage correction factors in the humerus, femur, radius, ulna, tibia, and fibula.

TABLE 4 | Dimensions of cartilaginous epiphyses compared to mineralized epiphyses. Values represent the percentage increase in long and short axes of the cartilaginous epiphyses over the mineralized epiphyses.

Species	Humeral head		Humeral condyles		Femoral head		Femoral condyles	
	Long axis	Short axis	Long axis	Short axis	Long axis	Short axis	Long axis	Short axis
<i>Ambystoma maculatum</i>	0.0%	0.0%	0.3%	7.6%	11.5%	11.5%	1.0%	0.0%
<i>Ambystoma mexicanum</i>	23.0%	46.4%	-1.0%	36.5%	40.1%	51.8%	6.7%	-8.8%
<i>Ambystoma tigrinum</i>	16.1%	19.9%	1.8%	31.1%	31.2%	37.7%	13.5%	5.2%
<i>Bolitoglossa porrasorum</i>	15.1%	0.0%	17.5%	19.5%	36.2%	26.0%	14.8%	53.8%
<i>Cryptobranchus alleganiensis</i>	28.5%	60.5%	1.2%	29.3%	51.0%	10.9%	17.6%	0.8%
<i>Hynobius nebulosus</i>	9.4%	21.2%	-2.1%	14.6%	14.5%	17.6%	3.7%	3.2%
<i>Necturus maculatus</i>	29.7%	55.1%	18.9%	24.7%	55.7%	63.5%	14.2%	-0.7%
<i>Plethodon cinereus</i>	0.0%	0.0%	3.1%	20.5%	4.9%	20.8%	18.1%	32.7%
<i>Pleurodeles waltl</i>	40.0%	65.2%	84.3%	61.7%	7.2%	34.0%	61.3%	18.2%
<i>Pseudotriton ruber</i>	17.3%	3.2%	-0.7%	4.8%	14.2%	17.1%	8.5%	26.7%
<i>Salamandra salamandra</i>	-0.1%	9.5%	4.6%	47.1%	42.0%	56.2%	10.5%	4.4%
<i>Siren intermedia</i>	26.6%	31.1%	16.9%	-2.3%	-	-	-	-
<i>Siren lacertina</i>	21.0%	49.0%	0.1%	26.7%	-	-	-	-
Average	17.4%	27.8%	11.1%	24.8%	28.0%	31.6%	15.5%	12.3%

are closely related and very similar in morphology and ecology, relative cartilage thickness was much greater in the lesser siren *S. intermedia* than in the greater siren *S. lacertina* (51% versus 31% in the humerus). The large variation present within extant salamanders increases the uncertainty of cartilage reconstruction in their extinct relatives.

The study was not designed to examine the effects of sexual maturity on cartilage thickness, but, because the process of cartilage erosion and bone deposition continues until adulthood (Sanchez et al., 2010b), it is likely that immature specimens have a greater percentage of cartilage. Similarly, negative allometry of cartilage thickness across ontogeny has been demonstrated in the long bones of *Alligator* (Holliday et al., 2010) and frogs (e.g., Erismis and Chinsamy, 2010). Two specimens, the terrestrial Pijol Salamander *Bolitoglossa porrasorum* and the semi-aquatic Iberian News *Pleurodeles waltl*, were substantially smaller than average length at sexual

maturity (Table 1), and both had unusually large cartilage correction factors in the humerus and femur for their mode of life (30.4–31.8% and 44–52%, respectively). However, excluding *B. porrasorum* from the analysis did not change the result that mean CCF is significantly larger in aquatic salamanders: the differences between aquatic and terrestrial salamanders were still significant, with marginally larger effect sizes ($t = 3.4-3.5$ versus $2.6-3.2$) and smaller p -values ($p = 0.015-0.016$ versus $0.022-0.037$) (*P. waltl* was not included in either analysis because it is classed as semi-aquatic). An additional specimen, the California Giant Salamander *Dicamptodon ensatus*, fell within the range of adult lengths but was excluded from the analysis because it retained a remnant of external gills and thus, as a facultative neotenic species (Wakahara, 1996), it could not be classified confidently as aquatic or terrestrial. This specimen had extraordinarily thick cartilage caps (97% in the humerus and 121% in the femur)

(Dao et al., 2020). An examination of larvae, juveniles, and adults of known age and reproductive status would be necessary to test the relationship between sexual maturity and cartilage thickness in salamanders.

Another limitation of the dataset is the relatively sparse sampling at the upper end of the body size range. The sample was restricted to specimens that were available for destructive testing from local museums or from colleagues, plus DiceCT scans available on Morphosource.com. The largest salamander in the sample is *C. alleghaniensis* (16 cm SVL), but this species can reach 40 cm SVL (Petranka, 1998; Raffaelli, 2014). The largest extant salamanders are the Chinese and Japanese Giant Salamanders (*Andrias davidianus* and *A. japonicus*, respectively), and males of these species can reach 102 cm total length (comparable to the Devonian stem tetrapod *Acanthostega*), though the average size of adults is much smaller (Kawamichi and Ueda, 1998). Unfortunately, large *Andrias* specimens are rare and none were available for DiceCT. However, a micro-CT scan without contrast reveals that, like those of *Cryptobranchus* and other aquatic neotenic salamanders, the mineralized portions of the humerus and femur in *Andrias japonicus* are concave at either end, presumably accommodating large cartilage cones (specimen from Florida Museum of Natural History, Amphibians and Reptiles: 31536; ark:/87602/m4/M77893; www.MorphoSource.org, Duke University). Therefore, a 30–50% CCF would be expected in *Andrias*, similar to the other aquatic salamanders. In addition to extra-large aquatic salamanders, the dataset lacks very large terrestrial salamanders. The largest terrestrial salamander in the sample is *S. Salamandra* at 7.7 cm SVL, although this species can reach 20–30 cm total length (Raffaelli, 2014). A specimen was acquired of the largest terrestrial salamander, the California Giant Salamander *Dicamptodon ensatus*, but, as explained above, it was excluded because it was incompletely metamorphosed. As DiceCT becomes more broadly available, future studies with greater sampling of large body sizes will be able to test whether or not the correlation between relative cartilage thickness and SVL is an artifact of the tendency toward larger body sizes in aquatic salamanders.

The girdles of salamanders contain varying amounts of cartilage, which was not measured for this study. Some, such as the Common Mudpuppy *N. maculatus*, have completely cartilaginous glenoids and acetabula, while others, such as the Red Salamander *P. ruber*, have bony glenoids and acetabula covered by a very thin layer of articular cartilage (Figures 1A–D). The cartilaginous component of the girdles would have little effect on limb length but a large effect on range of motion because in salamanders like *N. maculatus* cartilage makes up the entire glenoid and acetabulum. In addition, cartilaginous parts of the girdles provide the origins of muscles that attach to the limbs in all taxa (e.g., the cartilaginous suprascapula forms the origin of *m. dorsalis scapulae* [deltoideus]; Francis, 1934).

Comparison to Other Tetrapods

The epiphyseal structure of salamanders is unique among extant tetrapods, and articular cartilage makes up a larger proportion of the length of long bones in salamanders than in any other

tetrapod reported thus far. Mammals and lepidosaurs develop secondary centers of ossification and have very thin articular cartilage (Haines, 1942). Archosaurs and turtles do not have secondary ossification centers, but their epiphyses contain bony protrusions which play a similar mechanical role (Xie et al., 2020). Some frogs have epiphyses formed from calcified cartilage (Haines, 1942; Carter et al., 1998). Differences in the structure and composition of epiphyses are thought to relate to the presence or absence of mechanical stresses imposed by rapid growth in a terrestrial environment (Xie et al., 2020).

The humeri of salamanders have a cartilage correction factor almost four times as large as that of American Alligators, which have the greatest proportion of cartilage reported among archosaurs ($31 \pm 15\%$ versus $8 \pm 3\%$) (Holliday et al., 2010). In the femur, CCF was $26 \pm 10\%$ in salamanders compared to $6 \pm 2\%$ in alligators. The disparity was even more pronounced in the distal limb bones: average CCF in the radius, ulna, tibia, and fibula among the salamanders in this study ranged from 26 to 44%, while in alligators it ranged from 5 to 9%. Unlike in salamanders, the ulna in alligators did not have a particularly large CCF compared to the other long bones. Effect on width and breadth of epiphyses were comparable between the two groups. For example, articular cartilage added 13–27% to the craniocaudal and mediolateral dimensions of the humeral head in alligators (Holliday et al., 2010) and 17–28% to the corresponding dimensions (long and short axes, respectively) in salamanders. For comparison, in adult ostriches the CCF was only 2% in length of the humerus and 9–11% in the humeral head (Holliday et al., 2010).

Implications for Fossil Reconstruction

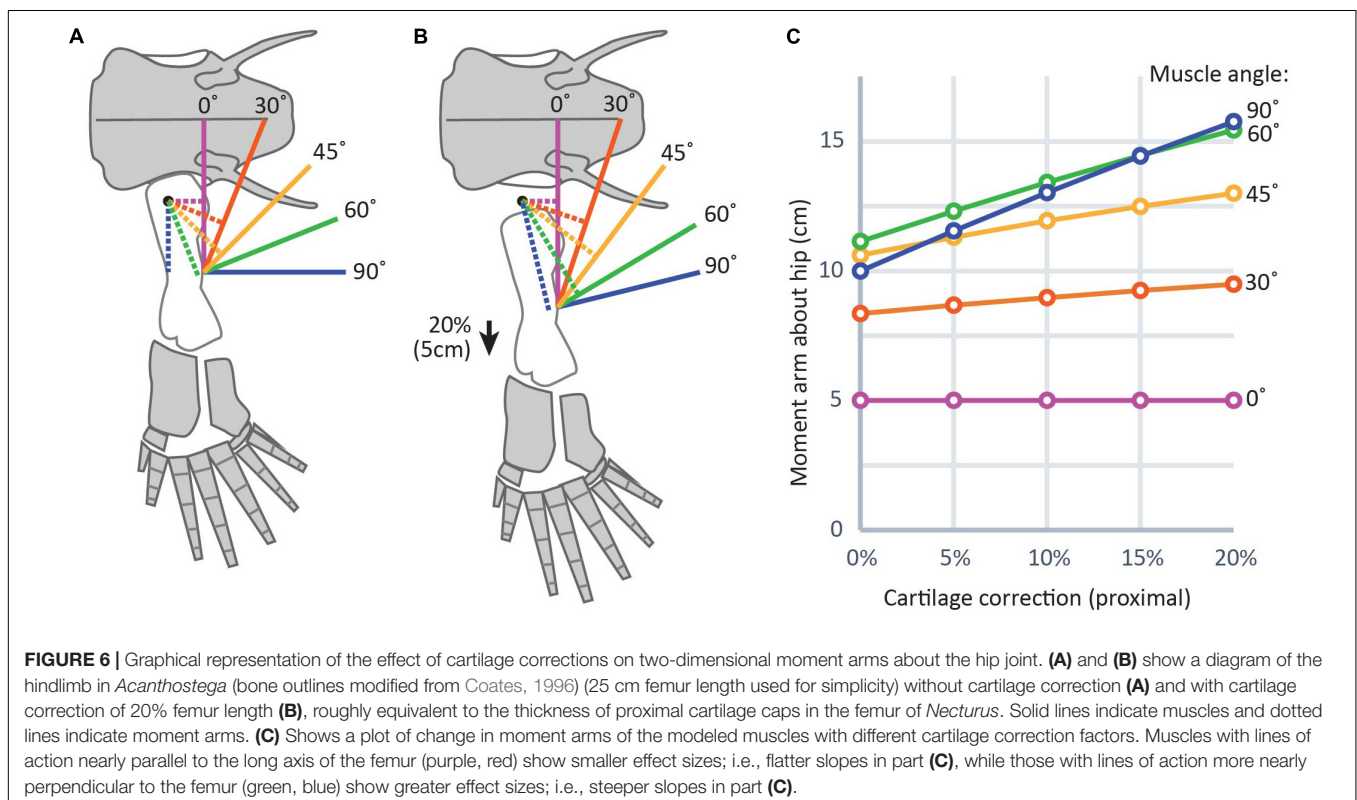
In addition to physical constraints, data from extant animals are one of the most valuable resources for placing bounds on uncertainty about unpreserved attributes (Witmer, 1995; Hutchinson, 2011). For example, the range of cartilage thickness in extant salamanders provides a reasonable starting point for estimating cartilage thickness in early limbed tetrapodomorphs because the two groups are similar in body proportions, mode of life, and, to some extent, the structure of the mineralized portions of their epiphyses. Even more valuable are data from extant animals within a phylogenetic context combined with osteological correlates in fossils (“extant phylogenetic bracket”; Witmer, 1995). Though beyond the bounds of the current study, identifying and tracing osteological correlates of various cartilage thicknesses in stem amphibians and stem amniotes would strengthen inferences about articular cartilage in stem tetrapods. Potential correlates of thick articular cartilage have been identified in extinct archosaurs, including rough, weakly convex articular surfaces that are not congruent with each other (Holliday et al., 2010; Tsai et al., 2020).

Relative cartilage thickness was very different between aquatic and terrestrial salamanders in this study, raising the question, which group is a better model for the first vertebrates with limbs? In many ways the aquatic group seems most appropriate because Devonian tetrapodomorphs with limbs such as *Acanthostega* and *Ichthyostega* probably were fully aquatic and shared features with neotenic salamanders such as functional gills and a large tail fin

(Coates and Clack, 1991; Clack and Coates, 1995; Clack et al., 2003). Like aquatic salamanders, stem tetrapods lacked a central marrow cavity (Estefa et al., 2021), possibly reflecting their habits; aquatic animals may benefit from having a larger amount of cartilage because cartilage is less brittle than bone and thus less likely to fracture, or because it is metabolically less costly to maintain (Haines, 1942), whereas a complete medullary cavity is thought to help accommodate the torsional loads incurred during terrestrial locomotion (Sanchez et al., 2010a). However, the unusual histological organization of the long bones of neotenic salamanders (described in the introduction) is thought to be a derived feature within urodeles (Haines, 1938, 1942). In contrast, the epiphyses of *Dicynodon* (a therapsid from the Upper Permian (Kammerer et al., 2011) contain a regular, radiate arrangement of bony trabecula similar to that found in turtles, crocodiles, and (to a lesser extent) in terrestrial salamanders, which Haines (1938, 1942) identified as the ancestral tetrapod condition. Recent work on *Acanthostega* and the closely related fishes *Eusthenopteron* and *Hyneria* describes a similar structure, with tubular marrow processes at the base of their epiphyses (Sanchez et al., 2014, 2016; Kamska et al., 2018). Therefore, even aquatic tetrapodomorphs may have had epiphyseal morphology and relative cartilage dimensions more like those of extant terrestrial salamanders, or even amniotes such as turtles and crocodiles (Haines, 1938; Estefa et al., 2021).

These results inform predictions about articular cartilage thickness in extinct animals in several ways. First, they help to predict differences among taxa by identifying traits that are correlated with thicker cartilage in salamanders and likely in their

extinct relatives (more aquatic habits, flat or convex mineralized epiphyses, and, possibly, sexual immaturity) and ones that are not (absolute body size and phylogenetic relatedness). Second, these results provide a starting point for determining cartilage correction factors in extinct taxa, which can then be used in a sensitivity analysis. Returning to stem tetrapods, a cartilage correction factor of $21 \pm 7\%$ in the femur could be used, corresponding to the mean and standard deviation in terrestrial salamanders in this study. These results can reasonably be applied to most stem tetrapods, with some caveats. Although often presented as a prototypical Devonian stem tetrapod, *Acanthostega* is not necessarily a good representative of the ancestral condition in terms of long bone histology and life history. Most notably, the degree of ossification in the humerus is seemingly unrelated to body size, and ossification did not begin until the animals reached nearly full size (Sanchez et al., 2016). This long delay in ossification might affect the ultimate size and shape of the cartilaginous epiphyses. In contrast, other Devonian and Early Carboniferous limbed vertebrates such as *Ichthyostega*, *Whatcheeria*, and *Pederpes* had more heavily ossified limb bones but appear to lack ossified or calcified epiphyses (Jarvik, 1996; Clack and Finney, 2005; Otoo et al., 2021), similar to extant salamanders. However, in *Pederpes* the ossified epiphyses are distinctly concave, suggesting very thick articular cartilage and an aquatic and/or juvenile condition (Clack and Finney, 2005). In contrast, terrestrial salamanders probably are not the best model for the epiphyses of many crown tetrapods. While prolonged juvenile stage is thought to be ancestral for limbed vertebrates (Sanchez et al., 2014, 2016; Kamska et al., 2018), some



stem amniotes such as *Seymouria* exhibited much faster bone growth than extant salamanders (Estefa et al., 2020), and the epiphyses of extant lepidosaurs might be a better analog. On the other extreme, some stem salamanders such as *Apateon* show pedomorphic growth patterns (Estefa et al., 2021) and might be more analogous to aquatic or semi-aquatic salamanders. One cautionary note: although no correlation between absolute size and cartilage thickness was observed in this study, many stem tetrapods [including *Acanthostega*, at approximately 60 cm total length (Coates, 1996), and *Ichthyostega*, which is slightly larger (Ahlberg et al., 2005)] fall outside the size range of the sampled taxa, producing some additional uncertainty.

The effect of unpreserved articular cartilage on range of motion in fossils is difficult to predict, and such a prediction was not attempted in this study. A preliminary study of the hindlimb of *Acanthostega* showed that a similar correction factor (cartilage cap 13% bone length on the proximal end; similar to the Fire Salamander *S. Salamandra*) would increase osteological range of motion of the hip by a modest 15–30° (Dao et al., 2020). However, this model assumes that cartilage is infinitely deformable and does not in itself restrict range of motion. Based on salamanders in the current study, the CCF for the length and width of the femoral head would be approximately 30% (Table 4), likely producing a more congruent hip joint and restricting range of motion. The results from these salamanders suggest that the dimensions of the femoral head are affected by articular cartilage to a greater degree than the humeral head, humeral condyles, or femoral condyles (although this varies among taxa).

Because adding a cartilage correction moves muscle insertion points distally further from their insertions, reconstructed muscle leverage would also be affected (Dao et al., 2020). Changes in muscle leverage will be greatest in muscles whose axes of movement are nearly perpendicular to the femur. In a model of a hindlimb with a 25 cm femur and a 20% CCF on the proximal end, slightly above the average for aquatic salamanders in this study (Figure 6), changes in moment arms of 4–6 cm were found for muscles that run nearly perpendicular to the femur, as opposed to those muscles whose axes were nearly parallel (0–2 cm). This result is logical: moving the insertion more distally (i.e., along the long axis of the bone) has the effect of lengthening a muscle whose line of action is parallel to the long axis of the femur but does not change its orientation (Figure 6, purple lines). However, for a muscle whose line of action is oblique to the femur, moving the insertion distally will both lengthen the line of action and change its orientation by decreasing the angle between the muscle and the femur (Figure 6, blue lines). Because a muscle's lever arm by definition is perpendicular to the line of action (e.g., Sherman et al., 2013), changing the orientation of the latter directly affects the former. Therefore, even without explicitly modeling moment arms it is possible to predict the effects of different assumptions about unpreserved articular cartilage on limb function. For example, our previous work on *Acanthostega* used a 7.5% CCF in the humeral head (Molnar et al., 2021). Had we used a CCF drawn from the average for terrestrial salamanders in this study (approximately 10%), the moment arms of shoulder retractors like latissimus dorsi and pectoralis posterior probably would have been several

centimeters larger, while those of elbow extensors such as triceps brachii would have been minimally affected.

DATA AVAILABILITY STATEMENT

The original contributions presented in the study are included in the article/**Supplementary Material**, further inquiries can be directed to the corresponding author/s.

ETHICS STATEMENT

Ethical review and approval was not required for the animal study because this research used only preserved specimens from existing collections.

AUTHOR CONTRIBUTIONS

JM conceived the study, collected and analyzed data, and wrote and edited the manuscript.

FUNDING

This project was supported by startup grant from NYIT to JM.

ACKNOWLEDGMENTS

I am grateful to Dan Gibbons for writing the MATLAB script, to Meredith Taylor for de-staining specimens, and to Kelsi Hurdle for assisting with micro-CT scanning. Access to the micro-CT scanner was provided with funding from NSF MRI 1828305. David Kizirian at the American Museum of Natural History and Michael Granatosky at NYIT provided specimens for scanning. Aki Watanabe performed a phylogenetic signal test in R and shared his contrast staining protocol, and the biomechanics research group at NYIT contributed ideas and feedback. Special thanks to Brandon Dao and Christine Chevalier-Horgan for the preliminary work that sparked this manuscript, and thanks to the two reviewers whose suggestions greatly improved it.

SUPPLEMENTARY MATERIAL

The Supplementary Material for this article can be found online at: <https://www.frontiersin.org/articles/10.3389/fevo.2021.671006/full#supplementary-material>

Supplementary Table 1 | Ancestor reconstruction of cartilage correction factors for humerus, femur, radius, ulna, tibia, and fibula using maximum parsimony

Supplementary Data Sheet 1 | MATLAB script for calculating two-dimensional moment arms with a cartilage correction factor.

Supplementary datasets | (available on MorphoSource.com upon publication): 15 DiceCT datasets representing the fore- and hindlimbs of various salamanders.

1. Right forelimb of *Pleurodeles waltl* (AMNH A168418)

2. Right hindlimb of *Pleurodeles waltl* (AMNH A168418)
3. Forelimbs of *Pseudotriton ruber* (NYIT MG1257)
4. Hindlimbs of *Pseudotriton ruber* (NYIT MG1257)
5. Forelimb of *Plethodon cinereus* (AMNH A159522)
6. Hindlimb of *Plethodon cinereus* (AMNH A159522)
7. Forelimbs of *Ambystoma tigrinum* (AMNH 26619)
8. Hindlimbs of *Ambystoma tigrinum* (AMNH 26619)

9. Forelimb of *Salamandra salamandra* (AMNH 26618)
10. Hindlimb of *Salamandra salamandra* (AMNH 26618)
11. Forelimbs of *Ambystoma mexicanum* (AMNH A144861)
12. Hindlimbs of *Ambystoma mexicanum* (AMNH A144861)
13. Forelimbs of *Siren lacertina* (AMNH A171810)
14. Forelimbs of *Necturus maculatus* (AMNH 26617)
15. Hindlimbs of *Necturus maculatus* (AMNH 26617)

REFERENCES

- Ahlberg, P. E., Clack, J. A., and Blom, H. (2005). The axial skeleton of the Devonian tetrapod *Ichthyostega*. *Nature* 437, 137–140. doi: 10.1038/nature03893
- AmphibiaWeb (2020). *Salamandra salamandra*: Fire Salamander. Available online at: <http://amphibiaweb.org/species/4284> (accessed Jan 26, 2021)
- Ashley-Ross, M. A. (2004). Kinematics of the transition between aquatic and terrestrial locomotion in the newt *Taricha torosa*. *J. Exp. Biol.* 207, 461–474. doi: 10.1242/jeb.00769
- Carter, D., Mikić, B., and Padian, K. (1998). Epigenetic mechanical factors in the evolution of long bone epiphyses. *Zool. J. Linn. Soc.* 123, 163–178.
- Clack, J., and Coates, M. I. (1995). *Acanthostega gunnari*, a primitive, aquatic tetrapod? *Bull. Muséum. Natl. Hist. Nat. Sect. C Sci. Terre. Paléontol. Géologie Minéralogie* 17, 359–372.
- Clack, J. A. (2012). *Gaining Ground: The Origin and Evolution of Tetrapods, Second*. Bloomington, IN: Indiana University Press.
- Clack, J. A., Ahlberg, P. E., Finney, S. M., Dominguez Alonso, P., Robinson, J., and Ketcham, R. A. (2003). A uniquely specialized ear in a very early tetrapod. *Nature* 425, 65–69. doi: 10.1038/nature01904
- Clack, J. A., and Finney, S. M. (2005). *Pederpes finneyae*, an articulated tetrapod from the Tournaisian of Western Scotland. *J. Syst. Palaeontol.* 2, 311–346. doi: 10.1017/S1477201904001506
- Coates, M. I. (1996). The Devonian tetrapod *Acanthostega gunnari* Jarvik: postcranial anatomy, basal tetrapod interrelationships and patterns of skeletal evolution. *Trans. R Soc. Edinb.* 87, 363–421.
- Coates, M. I., and Clack, J. A. (1991). Fish-like gills and breathing in the earliest known tetrapod. *Nature* 352, 234–236.
- Dao, B., Chevalier-Horgan, C. L., Pierce, S. E., and Molnar, J. L. (2020). The effect of cartilage thickness on reconstructions of range of motion and muscle leverage in extinct tetrapods. *FASEB J.* 34, 1–1.
- Erismis, U. C., and Chinsamy, A. (2010). Ontogenetic changes in the epiphyseal cartilage of *rana (Pelophylax) caralitana* (Anura: Ranidae). *Anat. Rec.* 293, 1825–1837. doi: 10.1002/ar.21241
- Estefa, J., Klembara, J., Tafforeau, P., and Sanchez, S. (2020). Limb-bone development of seymouriamorphs: implications for the evolution of growth strategy in stem amniotes. *Front. Earth Sci.* 8:97. doi: 10.3389/feart.2020.00097
- Estefa, J., Tafforeau, P., Clement, A. M., Klembara, J., Niedźwiedzki, G., Berruyer, C., et al. (2021). New light shed on the early evolution of limb-bone growth plate and bone marrow. *Elife* 10:e51581.
- Francillon-Vieillot, H., de Buffrénil, V., Castanet, J., Géraudie, J., Meunier, F. J., Sire, J. Y., et al. (1990). Microstructure and mineralization of vertebrate skeletal tissues. *Skelet. Biominer. Patterns Process. Evol. Trends* 1, 471–530.
- Francis, E. (1934). *The Anatomy of the Salamander*. Oxford: Clarendon Press.
- Goris, R. C., and Maeda, N. (2005). *Guide to the Amphibians and Reptiles of Japan*. Malabar, FL: Krieger Publishing Company.
- Haines, R. W. (1938). The primitive form of epiphysis in the long bones of tetrapods. *J. Anat.* 72, 323–343.
- Haines, R. W. (1942). The evolution of epiphyses and of endochondral bone. *Biol. Rev.* 17, 267–292.
- Hedges, S. B., Dudley, J., and Kumar, S. (2006). TimeTree: a public knowledge-base of divergence times among organisms. *Bioinformatics* 22, 2971–2972.
- Helmenstine, A. M. (2020). *All About the Axolotl (Ambystoma mexicanum)*. New York, NY: ThoughtCo.
- Holliday, C. M., Ridgely, R. C., Sedlmayr, J. C., and Witmer, L. M. (2010). Cartilaginous epiphyses in extant archosaurs and their implications for reconstructing limb function in dinosaurs. *PLoS One* 5:e13120. doi: 10.1371/journal.pone.0013120
- Hutchinson, J. R. (2011). On the inference of function from structure using biomechanical modelling and simulation of extinct organisms. *Biol. Lett.* 8, 115–118. doi: 10.1098/rsbl.2011.0399
- Hutchinson, J. R., Anderson, F. C., Blemker, S. S., and Delp, S. L. (2005). Analysis of hindlimb muscle moment arms in *Tyrannosaurus rex* using a three-dimensional musculoskeletal computer model: implications for stance, gait, and speed. *Paleobiology* 31, 676–701.
- Jannel, A., Nair, J. P., Panagiotopoulou, O., Romilio, A., and Salisbury, S. W. (2019). “Keep your feet on the ground”: simulated range of motion and hind foot posture of the middle jurassic sauropod *Rhoetosaurus brownei* and its implications for sauropod biology. *J. Morphol.* 280, 849–878. doi: 10.1002/jmor.20989
- Jarvik, E. (1996). The Devonian tetrapod *Ichthyostega*. *Foss. Strata*. 40, 1–207.
- Joven, A., Kirkham, M., and Simon, A. (2015). “Husbandry of Spanish ribbed newts (*Pleurodeles waltl*)” in *Salamanders in Regeneration Research*, eds A. Kumar and A. Simon (New York, NY: Springer), 47–70.
- Kammerer, C. F., Angielczyk, K. D., and Fröbisch, J. (2011). A comprehensive taxonomic revision of *Dicynodon* (Therapsida, Anomodontia) and its implications for dicynodont phylogeny, biogeography, and biostratigraphy. *J. Vertebr. Paleontol.* 31, 1–158. doi: 10.1080/02724634.2011.627074
- Kamska, V., Daeschler, E., Downs, J., Ahlberg, P. E., Tafforeau, P., and Sanchez, S. (2018). Long-bone development and life-history traits of the Devonian tristichopterid *Hyeria lindae*. *Earth Environ. Sci. Trans. R Soc. Edinb.* 109, 1–12. doi: 10.1017/S175569101800083X
- Kawamichi, T., and Ueda, H. (1998). Spawning at nests of extra-large males in the giant salamander *Andrias japonicus*. *J. Herpetol.* 32, 133–136.
- Kawano, S. M., and Blob, R. W. (2013). Propulsive forces of mudskipper fins and salamander limbs during terrestrial locomotion: implications for the invasion of land. *Integr. Comp. Biol.* 53, 1–12. doi: 10.1093/icb/ict051
- Klitz, J. H. (1912). Die enchondrale Ossifikation bei den Amphibien (*Salamandra maculosa* Laur.). *Arb. Ueber. Zool. Inst. Wien.* 19, 165–194.
- Lannoo, M. J. (2005). *Amphibian Declines: The Conservation Status of United States Species*. Berkeley, CA: University of California Press.
- Lynn, W. G. (1961). Types of amphibian metamorphosis. *Am. Zool.* 1, 151–161.
- Marjanović, D., and Laurin, M. (2014). An updated paleontological timetree of lissamphibians, with comments on the anatomy of Jurassic crown-group salamanders (Urodela). *Hist. Biol.* 26, 535–550.
- Metscher, B. D. (2009). MicroCT for comparative morphology: simple staining methods allow high-contrast 3D imaging of diverse non-mineralized animal tissues. *BMC Physiol.* 9:11. doi: 10.1186/1472-6793-9-11
- Molnar, J. L., Hutchinson, J. R., Diogo, R., Clack, J. A., and Pierce, S. E. (2021). Evolution of forelimb musculoskeletal function across the fish-to-tetrapod transition. *Sci. Adv.* 7:eabd7457.
- Nafis, G. (2018). *A Guide to the Amphibians and Reptiles of California*. Corvallis, OR: California Herps.
- Najbar, A., Konowalik, A., Halupka, K., Najbar, B., and Ogielska, M. (2020). Body size and life history traits of the fire salamander *Salamandra salamandra* from Poland. *Amphib. Reptil.* 41, 63–74. doi: 10.1163/15685381-20191135
- Otoo, B. K. A., Bolt, J. R., Lombard, R. E., Angielczyk, K. D., and Coates, M. I. (2021). The postcranial anatomy of *Whatcheeria deltae* and its implications for the family Whatcheeridae. *Zool. J. Linn. Soc.* zlaa182. doi: 10.1093/zoolin/zlaa182
- Petranka, J. W. (1998). *Salamanders of the United States and Canada*. Washington, DC: Smithsonian Institution Press.

- Pierce, S. E., Hutchinson, J. R., and Clack, J. A. (2013). Historical perspectives on the evolution of tetrapodomorph movement. *Integr. Comp. Biol.* 53, 209–223.
- Quilhac, A., de Ricqlès, A., Lamrous, H., and Zylberberg, L. (2014). Globuli ossei in the long limb bones of *Pleurodeles waltl* (Amphibia, Urodela, Salamandridae). *J. Morphol.* 275, 1226–1237. doi: 10.1002/jmor.20296
- Raffaëlli, J. (2014). *Les Urodèles du Monde*, 2nd Edn. McLean, VA: Penden.
- Revell, L. J. (2012). phytools: an R package for phylogenetic comparative biology (and other things). *Methods Ecol. Evol.* 3, 217–223.
- Sanchez, S., Germain, D., De Ricqlès, A., Abourachid, A., Goussard, F., and Tafforeau, P. (2010a). Limb-bone histology of temnospondyls: implications for understanding the diversification of palaeoecologies and patterns of locomotion of Permo-Triassic tetrapods. *J. Evol. Biol.* 23, 2076–2090. doi: 10.1111/j.1420-9101.2010.02081.x
- Sanchez, S., Klembara, J., Castanet, J., and Steyer, J. S. (2008). Salamander-like development in a seymouriamorph revealed by palaeohistology. *Biol. Lett.* 4, 411–414. doi: 10.1098/rsbl.2008.0159
- Sanchez, S., Ricqlès, A. D., Schoch, R., and Steyer, J. S. (2010b). Developmental plasticity of limb bone microstructural organization in Apateton: histological evidence of paedomorphic conditions in branchiosaurs. *Evol. Dev.* 12, 315–328. doi: 10.1111/j.1525-142X.2010.00417.x
- Sanchez, S., Tafforeau, P., and Ahlberg, P. E. (2014). The humerus of Eusthenopteron: a puzzling organization presaging the establishment of tetrapod limb bone marrow. *Proc. R. Soc. B Biol. Sci.* 281:20140299. doi: 10.1098/rspb.2014.0299
- Sanchez, S., Tafforeau, P., Clack, J. A., and Ahlberg, P. E. (2016). Life history of the stem tetrapod *Acanthostega* revealed by synchrotron microtomography. *Nature* 537:408.
- Sherman, M. A., Seth, A., and Delp, S. L. (2013). “What is a moment arm? Calculating muscle effectiveness in biomechanical models using generalized coordinates,” in *Proceedings of the ASME Engineering Technical Conferences V07BT10A052* (New York, NY: American Society of Mechanical Engineers).
- Tsai, H. P., Middleton, K. M., Hutchinson, J. R., and Holliday, C. M. (2020). More than one way to be a giant: convergence and disparity in the hip joints of saurischian dinosaurs. *Evolution* 74, 1654–1681.
- von Eggeling, H. (1869). *Der Aufbau der Skeletteile in den Freien Gliedmassen der Wirbeltiere; Untersuchungen an Urodelen Amphibien*. Jena: Fischer.
- Wakahara, M. (1996). Heterochrony and neotenic salamanders: possible clues for understanding the animal development and evolution. *Zoolog. Sci.* 13, 765–776. doi: 10.2108/zsj.13.765
- Witmer, L. M. (1995). “The extant phylogenetic bracket and the importance of reconstructing soft tissues in fossils,” in *Functional Morphology in Vertebrate Paleontology*, ed. J. J. Thomason (Cambridge, MA: Cambridge University Press), 19–33.
- Xie, M., Gol’din, P., Herdina, A. N., Estefa, J., Medvedeva, E. V., and Li, L. (2020). Secondary ossification center induces and protects growth plate structure. *eLife* 9:e55212. doi: 10.7554/eLife.55212

Conflict of Interest: The author declares that the research was conducted in the absence of any commercial or financial relationships that could be construed as a potential conflict of interest.

Copyright © 2021 Molnar. This is an open-access article distributed under the terms of the Creative Commons Attribution License (CC BY). The use, distribution or reproduction in other forums is permitted, provided the original author(s) and the copyright owner(s) are credited and that the original publication in this journal is cited, in accordance with accepted academic practice. No use, distribution or reproduction is permitted which does not comply with these terms.